Review

Renewable Electricity for Decarbonisation of Road Transport: Batteries or E-Fuels?

Gianluca Pasini , **Giovanni Lutzemberger** and **Lorenzo Ferrari** *

Department of Energy, Systems, Territory and Constructions, University of Pisa, 56122 Pisa, Italy
* Correspondence: lorenzo.ferrari@unipi.it; Tel.: +39-050-2217132

Abstract: Road transport is one of the most energy-consuming and greenhouse gas (GHG) emitting sectors. Progressive decarbonisation of electricity generation could support the ambitious target of road vehicle climate neutrality in two different ways: direct electrification with onboard electrochemical storage or a change of energy vector with e-fuels. The most promising, state-of-the-art electrochemical storages for road transport have been analysed considering current and future technologies (the most promising ones) whose use is assumed to occur within the next 10–15 years. Different e-fuels (e-hydrogen, e-methanol, e-diesel, e-ammonia, E-DME, and e-methane) and their production pathways have been reviewed and compared in terms of energy density, synthesis efficiency, and technology readiness level. A final energetic comparison between electrochemical storages and e-fuels has been carried out considering different powertrain architectures, highlighting the huge difference in efficiency for these competing solutions. E-fuels require 3–5 times more input energy and cause 3–5 times higher equivalent vehicle CO_2 emissions if the electricity is not entirely decarbonised.

Keywords: road transport; decarbonisation; renewable electricity; electrochemical storage; battery electric vehicle; Power-to-X; hydrogen; e-fuel; powertrain; greenhouse gas emission

1. Introduction

On 15 November 2022, the world population hit 8 billion [1]. Meanwhile, the 27th United Nations Framework Convention on Climate Change Conference of Parties (COP27) took place in Egypt. With record-high greenhouse gas levels, a surging energy crisis, and severe weather events across the world, COP27 aimed to achieve the goals of the Paris Agreement and limit global warming to 1.5 degrees Celsius with respect to preindustrial levels [2,3].

The transport sector accounts for a significant share of greenhouse gases (GHG) emitted globally. Many papers and reports of international agencies periodically analyse and publish data on the impact of different sectors. The world's final energy demand in 2020 was 410 EJ (113889 TWh) with transport responsible for almost 25%: about 100 EJ (27778 TWh). In 2019, the last year before the global pandemic effect, transport consumed almost 120 EJ globally with a continuous increase in the last decades [4].

Data published in 2022 by Eurostat [5] and reported in Figure 1 reveal that in advanced countries, transport is even more impactful than other single sectors with almost 30% of final energy consumption. The evolution of EU27 transport consumption in the last three decades has been rather discontinuous, with constant growth until 2007 followed by a recessionary phase caused by the global financial crisis of 2008 until 2013, and only since 2014 has consumption returned to reach precrisis levels only in 2019. The final energy consumption in transport was 289 Mtoe (3361 TWh) in 2019 and 252 Mtoe (3012 TWh) in 2020. In 2020, consumption fell due to the global COVID-19 pandemic and lockdown measures, but preliminary data for 2021 showed a remarkable bounce partially held back in 2022 by Ukraine's war and the consequent global energy crisis. The authors decided to

analyse the most updated data on road transport before these events, assuming that the global use of road transport, energy, and the market will return to precrisis levels.

(**a**) (**b**)
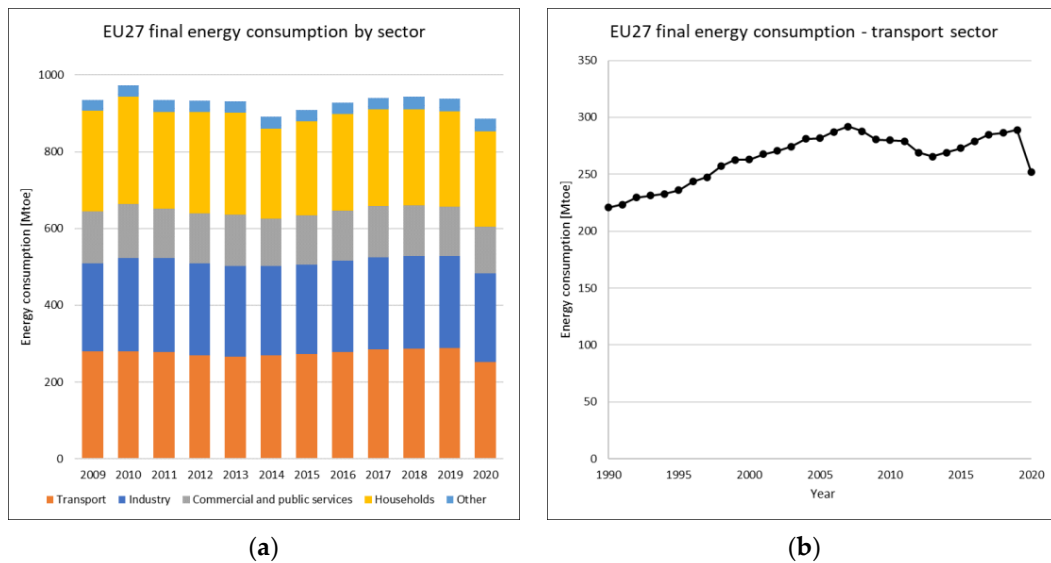
Figure 1. EU27 energy consumption by sector and focus on the last 30 years of transport.

Road transport includes many different types of vehicles from small two-wheelers to long-haul trucks with huge differences in terms of efficiency, power, and energy density requirements. The Italian Institute for Environmental Protection and Research (ISPRA) 2021 published a study on national GHG emissions with interesting elaborations regarding road transport [6]. In Figures 2 and 3, Italian 2019 fuel consumption and total mileage are split into vehicle type and driving area: passenger cars (PC) absolutely take the lion's share, but also light commercial vehicles (LCV) and heavy-duty trucks (HDT) show a remarkable consumption despite smaller mileages. PCs and LCVs are mainly used in rural areas, while buses and HDTs are used on highways, and two-wheelers are mainly in urban areas. Such detailed data are not available for the EU or at a global level, but the Italian scenario is representative of that of other Western countries.
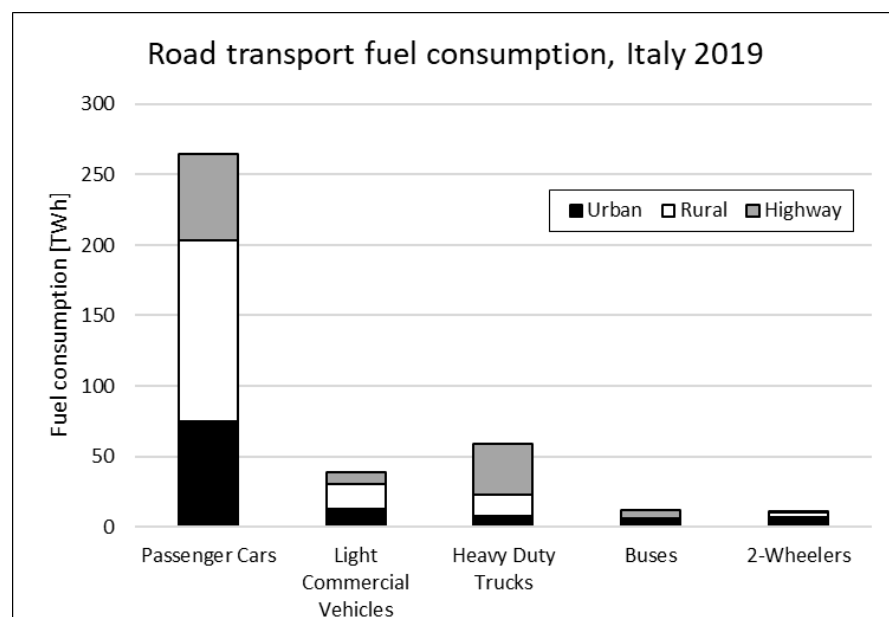
Figure 2. Road transport fuel consumption in Italy 2019.
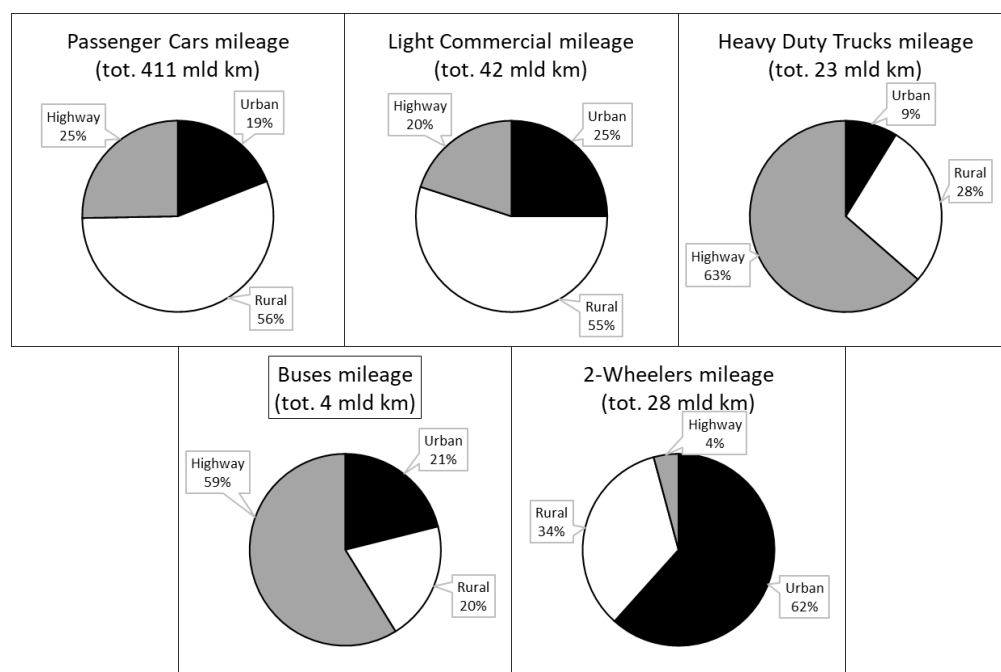
Figure 3. Road transport mileage and driving areas in Italy 2019.

From consumption and mileage data [6,7], the average consumption of the different categories of vehicles can be estimated. For the sake of simplicity, these categories have been divided into spark-ignited (SI) and compression-ignited (CI), including the few CNG and LPG vehicles in the SI category. Considering energy densities (34.2 MJ/L for SI vehicles and 38.6 MJ/L for CI vehicles, assuming gasoline and diesel as the dominant fuels), the average consumption for each vehicle in l/100 km and kWh/100 km is calculated and shown in Table 1. Then, using the fuel emission factors (2.34 $kgCO_2$/l for gasoline and 2.61 $kgCO_2$/L for diesel), the average gCO_2/km is obtained. These values figure out the great variability of consumption of the circulating fleet but also highlight the difference between real driving behaviour and the limits imposed by the legislator for vehicle homologation.

Table 1. Road transport specific fuel consumption and CO_2 emission in Italy 2019.

	Fuel Consumption [L/100 km]				Fuel Consumption [kWh$_{fuel}$/100 km]	CO_2 Emission [gCO_2/km]
	Urban	**Rural**	**Highway**	**Total**		
Passenger Cars SI	10.58	5.63	6.26	6.90	65.6	161
Passenger Cars CI	8.41	5.43	5.48	5.93	63.6	155
Light Commercial Vehicles SI	18.28	7.71	7.44	10.30	97.8	241
Light Commercial Vehicles CI	11.40	7.05	9.22	8.57	91.9	224
Heavy Duty Trucks CI	33.95	21.71	22.73	23.43	251.2	611
Buses SI	56.98	38.21	-	55.12	523.7	1290
Buses CI	38.37	24.79	20.91	24.79	265.8	647
2-wheelers SI	4.14	3.58	4.66	3.97	37.7	93

Switching from energy consumption to GHG emission, the whole energy sector contributes 76.2%, and road transport is responsible for a significant portion (12.5% of total GHG without emissions related to vehicle manufacturing and other transport equipment included in the industry sector), while aviation and naval shipping reach 2.1% and 1.8%, respectively [8].

Emissions from road transport come from the onboard use of diesel, gasoline, and natural gas in internal combustion engines (direct emissions) and a minimal part from electricity generation for electrified vehicles (indirect emissions). Globally, about 60% of

GHG is emitted by passenger transport (cars, two-wheelers, buses) and 40% by freight transport (commercial and heavy vehicles) [9].

In 2020, the EU vehicle fleet was composed of 246.3 million PCs, 29 million LCVs, 6.2 million HDTs, and almost 0.7 million buses. The average vehicle age is well above a decade: PCs are on average 11.8 years old, LCVs 11.9, HDTs 13.9, and buses 12.8. The fleet of HDTs, LCVs, and buses is dominated by diesel fuel, while the PC fleet is split between gasoline and diesel (51.7% and 42.8%) with a small share of alternative powertrains [10]. Despite the current small penetration in the existing fleet of PCs, the electric car (BEVs and PHEVs) EU market share is rapidly increasing. There was a dramatic increase in the number of new registrations from a few hundred in 2010 to about a million units in 2020 when they accounted for 11% of new registrations. In 2021, the total rose to 1.7 million with BEVs accounting for 9.0% of total new car registrations, while plug-in HEVs represented 8.8% with a sum of almost 18%. [11].

The decarbonisation of other energy sectors, in particular, electricity generation, has successfully reduced CO_2 emissions over the last decades, and the pathway to high renewables penetration nowadays is clear: the EU with its 'European Green Deal' aims to be climate-neutral by 2050, and the European Climate Law of 2021 sets a legally binding target [12]. Recent EU legislation sets targets to cut CO_2 emissions from PCs by 55% and LCVs by 50% by 2030. [13]. It also proposes to further cut emissions from these categories by 2035, effectively banning the sale of new fossil fuel cars from 2035.

In the EU, there are also other limits, the so-called 'Euro X' standards, for air pollution from road transport, including harmful emissions such as nitrogen oxides (NOx) and particulate matter (PM). The European Commission in November 2022 presented a proposal of Euro7 limits to reduce air pollution from new road vehicles sold in the EU, tackling emissions from tailpipes, brakes, and tires. The proposed rules are technology neutral, placing the same limits regardless of whether the vehicle uses gasoline, diesel, electricity, or other fuels [14].

RESs such as solar and wind are unreliable and inconsistent during generation, making it challenging to use them continuously and stably. One solution to this problem is to use energy storage systems [15], which could significantly enhance the utilisation and stability of RES electricity generation. Road transport represents a new potential electrical load (for battery recharging or e-fuel production) for national systems.

Road transport, which lags behind other sectors, could benefit from the decarbonisation of electricity generation in two different ways: direct electrification with battery electric vehicles (BEV) or the use of fuels produced with electricity (e-fuels). BEVs have zero local pollutants, such as NOx, NH_3, CO, Tand HC, and PM (except for the PM coming from tyre wear), while e-fuels still generate harmful emissions during onboard conversion.

2. Powertrain Architectures

According to the International Standardisation Organisation [16], a battery electric vehicle (BEV) is an electrically propelled vehicle with only a traction battery as a power source for vehicle propulsion. Instead, a hybrid vehicle presents at least two, or several, energy sources installed onboard, having a minimum one path of reversible energy flow between an energy source and the wheels and a minimum one path of energy flow which is not reversible.

To make practice considerations, thus limiting the generality of definition, it is possible to focus attention on the configuration depicted in Figure 1:

- Two onboard energy sources.
- The source that generates energy (mechanical or electric) from fuel (gasoline, natural gas, or hydrogen), here called 'fuelled source' (FS), has a single-direction energy flow (depicted in the figure as a one-way red arrow below P1).
- The additional source is one rechargeable energy storage system (RESS) that can deliver or store energy. The available energy is typically much lower than that coming

from the fuelled source, and the power flow is necessarily bidirectional (depicted in the picture as two-way red arrows near the black lines).

The scheme shown in Figure 4 does not describe the way to combine different powers from the two sources. Hybrid vehicles can be divided into several typologies. A general classification is the following: series hybrid electric vehicles (S-HEVs), where the sum of the power from the two sources is electrical; parallel hybrid electric vehicles (P-HEV), in which the sum of the power from the two sources is mechanical; complex hybrid electric vehicles (C-HEVs): all the other types in which the sum of the power from the two sources is made in several ways. When one source is a fuel-cell system, the vehicle is a fuel-cell hybrid electric vehicle (FC-HEV). Although a fuel-cell system (FCS) could also be used without the presence of an RESS, this is one very common configuration since an FCS is typically not suitable for rapid load-changing conditions [17] and can be significantly downsized. Moreover, an RESS can manage the peak powers requested by the load. In all cases, a *plug-in option* is mentioned, referring to the possibility of also recharging the RESS from the grid.
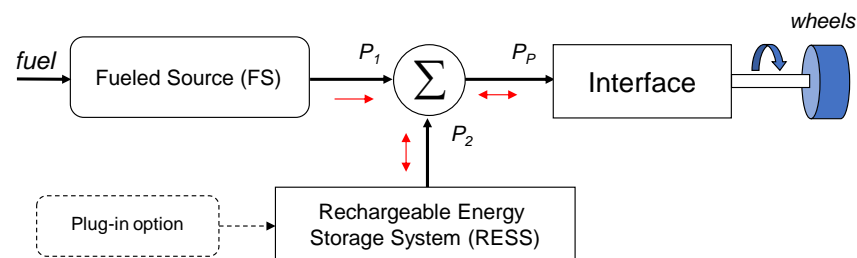
Figure 4. General architecture of a hybrid vehicle.

3. Batteries

3.1. Economic Investments

One of the most useful indicators regarding the technological evolution of batteries is the amount of economic investments from different countries. In mid-2021, China released its five-year plan in which it focused R&D efforts for the future generation of battery chemistries. In particular, they would like to invest in the development of the Na-ion battery industry during the period 2021–25 to achieve large-scale production, lower costs, and improved battery performance [18].

The European Union has a strategy for the development of internal battery supply chains. In this regard, the European Battery Alliance [18] and US Li-Bridge Alliance started cooperating to promote the development of Li-ion and the next generation of batteries, also considering raw materials. Additionally, the Important Projects of Common European Interest (IPCEI) [18] is a key strategy towards the implementation of that strategy. The Batt4EU [18] Partnership, started in 2021, combines efforts from the European Commission and members of several associations, which include industry and R&D stakeholders [18].

Moreover, the United States have several initiatives: One includes the release of the National Blueprint for Lithium Batteries, which elaborates one vision to include secure materials and technology supply chains in terms of raw and critical materials; creating domestic electrode, cell, and pack manufacturing; and recycling. In 2021, the US Department of Energy Argonne National Laboratory [18] created Li-Bridge, a new partnership to overcome gaps in the internal lithium supply chain.

Other initiatives came from Canada, India, Japan, Korea, and Southeast Asia towards the promotion of generic battery research and innovation [18]. All investments from countries and public entities continue to consider lithium-based technologies to the maximum extent, with some consideration of new specific technology, such as Na-Ion batteries. Other innovative technologies, which will later be mentioned, have been mostly developed by start-ups and small companies.

3.2. Lithium Batteries

Many types of lithium batteries exist on the market. They are often referred to by a three-letter acronym; the basic constitution of some of the most common types is illustrated in Table 2. Note that all types except LTO have graphite-based negative terminals (anode). Values of specific power/energy and power/energy density taken from some existing manufacturers [19–36], updated in 2022, are also shown in Table 2. The table shows that even within the same family, e.g., NMC, different products are available (even from the same manufacturer) with different characteristics. As is visible, different chemistries have different characteristics. Even inside the same chemistry, significant differences may occur. For instance, the same important manufacturer produces several types of NMC cells, in particular, high-energy, high-power, and super-high-power types. The situation depicted in Table 2 is up-to-date at the present time, with all the products currently available. It must also be mentioned that lithium technology remains today the most effective, practical, and reliable electrochemical storage solution. Different technologies, such as metal–air, sodium-ion, and solid-state batteries, although having some interesting characteristics, cannot be considered at the same development stage. However, these will be briefly introduced in subsequent sections to let the reader know the most promising solutions expected in the next decades.

Table 2. Selection of most common lithium-based chemistry types on the market (2022).

Chemistry Type	"+" Pin Material	"-" Pin Material	Specific Energy (Wh/kg)	Energy Density (Wh/L)	Specific Power (W/kg)	Power Density (W/L)
Li-Co Oxide (LCO)	$LiCoO_2$	Graphite	200 [19] 222 [20]	580 [19] 631 [20]	400 [19] -	1100 [19] -
Li-Mn Oxide (LMO)	$LiMn_2O_4$	Graphite	157 [21] 78 [22]	317 [21] 114 [22]	- 480 [22]	- 700 [22]
Li-Ni-Mn-Co Oxide (NMC)	$LiNiMnCoO_2$	Graphite	146 [23] 192 [24] 230 [25] 160 [26] 165 [27] 250 [28]	270 [23] 410 [24] 650 [25] 436 [26] 356 [27] 707 [28]	560 [24] 1500 [25] 2100 [23] 1777 [26] 1666 [27] 943 [28]	1200 [24] 3800 [23] 4400 [25] 4850 [26] 3608 [27] 2660 [28]
Li-Ni-Co-Al Oxide (NCA)	$LiNiCoAlO_2$	Graphite	200 [29] 207 [30]	460 [29] 545 [30]	- 1500 [30]	- 4000 [30]
Li-Fe Phosphate (LFP)	$LiFePO_4$	Graphite	86 [31] 108 [32] 124 [33] 166 [34]	140 [31] 240 [32] 240 [33] 362 [34]	860 [31] 2600 [32] 340 [33] 500 [34]	1400 [31] 5700 [32] 660 [33] 1088 [34]
Li-Ti Oxide (LTO)	-	$Li_4Ti_5O_{12}$	46 [35] 80 [36]	82 [35] 190 [36]	1600 [36] 2800 [35]	3600 [36] 4900 [35]

3.3. Metal–Air Batteries

Metal–air batteries (MABs) are safer and have a higher energy density than other types. The utilisation of oxygen from ambient air as a cathode (positive electrode) source has the additional benefit of reducing cost and weight considerably. Furthermore, the anode (negative electrode) of the MAB may be constructed from low-cost materials [37]. Different chemistries, each with their pros and cons, are possible for this type of battery. The main ones are shown below.

- *Mg-air*: Mg-air systems are attractive because of the uniform deposition of Mg metal; however, this type of device suffers regarding electrochemical instability. In addition, the corrosion of the Mg electrode severely restricts the use of aqueous electrolytes [37].

- *Al-air*: Aluminium-air-based batteries turn out to have promising chemistry. Firstly, aluminium is abundant in nature and relatively safe to handle. Furthermore, this type of chemistry is characterised by a high theoretical energy density and high specific energy values [38].
- *Na-air*: The great abundance in nature and the lithium-like characteristics have promoted the research of this type of chemistry. However, the development of these systems is still in its early stage [37].
- *Si-air*: Silicon is the second most abundant element in the earth's crust, and its semiconductor characteristics make it an attractive candidate for electronic applications [39]. Si-air batteries have a high theoretical energy density; however, they have problems with efficiency, reversibility, and corrosion. In particular, the reversibility of the system has not yet been demonstrated due to the stability of the silicon oxide (SiO_2) and silicate compounds in alkaline solutions. Moreover, silicon is corroded during the discharge phase, especially in alkaline solutions [37,39].
- *Li-air*: They appear to be the most promising of the metal–air systems currently studied. A lithium metal electrode is expected to reach high energy densities since it is a very electropositive (-3.04 V) and light (0.53 g/cm^3) material that is also characterised by a high specific capacity (3860 Ah/kg). Unfortunately, however, the contact of metallic lithium with a liquid electrolyte is extremely problematic due to the high reactivity of lithium both with solvents and with the salts contained in the electrolyte. The surface of the lithium in contact with the electrolyte forms the so-called solid electrolyte interphase (SEI), i.e., it transforms into a porous mosaic structure of insoluble lithium compounds with a consequent loss of the lithium available for the electrochemical reaction and a reduction of the life of the cell with the risk of the formation of dendrites, which remains a crucial point for the optimal functioning of lithium–air batteries [40]. Despite the difficulties, this type of battery looks promising [37].
- *Zn-air*: Zn-air rechargeable batteries are promising energy sources using inexpensive and environmentally friendly materials [40]. Zinc-air batteries (ZABs) are the only developed metal–air system today available, and they have been successfully marketed as primary cells for many decades [37]. One of the advantages of this system, unlike other chemicals such as lithium-based ones, is its stability in water. Their lifespan and electrical rechargeability, on the other hand, are significantly limited [37]. Current research attempts to increase the lifespan of these devices and improve their effectiveness.
- *Fe-air*: Fe-air batteries have been mainly studied as a rechargeable power supply system for electric vehicles. The theoretical specific energy is 1000 Wh/kg using oxygen present in the air as a positive electrode; unfortunately, at present, the specific energy that can be obtained is about 10% of the expected value [38]. Currently, other research aims to reduce the self-discharge problems of these systems in an alkaline environment, improve the reversibility of discharge products, and improve general performance [39].

Some properties of the most common types are shown in Table 3. As anticipated, despite having some interesting characteristics, metal–air batteries do not seem to be ready for a massive market entry. In fact, the data in Table 3 relate mainly to laboratory demonstrators, have no homogeneous characteristics (e.g., the extremely reduced cycling life vs. the extremely high value of specific energy), and are not designed for mass production. However, some pilot projects related essentially to stationary applications are currently going on [41], leaving room for future improvements and development for other fields of application (e.g., automotive). Apart from the cited reference, no other demonstrators are currently known. Clearly, the availability of market products is also missing.

Table 3. Selection of most common metal–air chemistry types.

Chemistry Type	Specific Energy (Wh/kg)	Energy Density (Wh/L)	Specific Power (W/kg)	Cycles
Al-air	300–500 [37] 500 [38] 925 [38]	1350 [38] 1692 [38]	-	-
Li-air	362 [38] 1700 [37]	194 [38]	-	75 [42] >250 [37]
Zn-air	90–120 [18] 300 [38] 350–500 [37]	2150 [38]	-	>75 [37]
Na-air	1600 [37]	-	300 [37]	40 [37] >20 [37]
Mg-air	400–700 [37] 3900 [37]	14,000 [37]	-	<10 [37]
Fe-air	50–75 [37] 300–500 [39]	-	-	3500 [37]
Si-air	140 [39] 1600 [39]	-	-	-
Sn-air	860 [37]	-	-	-

3.4. Sodium-Ion (Na-Ion) Batteries

A sodium-ion (Na-ion) battery is a rechargeable battery that uses sodium ions as charge carriers. Currently, several start-up companies are developing different sodium-ion-based technologies. As for metal–air batteries, this technology cannot be considered consolidated yet. However, in recent years, a large manufacturer [43] entered the market and declared some interesting features (e.g., specific energy around 160 Wh/kg) and the development of a basic industrial chain by 2023.

Among start-up companies, one of the most promising is Natron Energy, which focused on the use of Prussian blue analogues (PBA). The Natron sodium-ion cell contains different PBA materials. The cathode is an iron-based material, i.e., $Na_xM_yFe(CN)_6 \cdot nH_2O$, where M is a transition metal cation. On the anode side, the active material is sodium manganese hexacyanomanganate with a chemical formula of $Na_xMn_yMn(CN)_6 \cdot nH_2O$ [44].

According to Natron Energy, the complete assembly of PBA-based Na-ion batteries can be manufactured in any Li-ion production plant, starting from stacking up to the sealing process. Natron Energy is currently working on scaling up this technology [44].

PBA-based Na-ion batteries have the advantage of using available raw materials, resulting in high sustainability. In addition, they demonstrated no thermal runaway in the test UL 9540A standard protocol, which is desired for safety-critical applications. In terms of performance, PBA-based Na-ion batteries are characterised by a power density of up to 1250 W/kg, which is higher than most Li-ion batteries (typically <1000 W/kg). Furthermore, they are theoretically able to withstand the highest number of cycles among all batteries (>40,000 cycles); in fact, Natron sodium-ion cells show a capacity loss of only 2% after 4 200 cycles, measured at 10C/10C, 25 °C and a 100% depth of discharge (DOD). The main drawback of this type of battery is the very reduced specific energy achieved, in particular, 23 Wh/kg at the cell level and 10.3 Wh/kg at the module level [44], although other manufacturers have declared, as said, much higher specific energy levels [43]. In Table 4 main characteristics of Na-ion batteries are reported.

In conclusion, Natron PBA-based sodium-ion batteries have put forth evidence of intermediate performance with respect to lithium-ion batteries and supercapacitors. Their sodium-ion technology shows maturity and competitiveness for high-power applications, such as backup power for data centres or regenerative braking. The commercial diffusion of

PBA-based battery could be the first sodium-ion battery product, then followed by others, thus creating an alternative to lithium-ion batteries [44].

Definitely, despite always being at the demonstrator level, this solution seems the closest to market, mainly due to the declaration by the large manufacturer already mentioned [43].

Table 4. Main characteristics of Na-ion chemistry.

Chemistry Type	Specific Energy (Wh/kg)	Energy Density (Wh/L)	Specific Power (W/kg)	Power Density (W/L)	Cycles
Na-ion	160 [43] 10 [44] [1] 23 [44] [2]	-	1250	350	>40,000

[1] Module level. [2] Cell level.

3.5. Solid-State Batteries

One of the promising systems able to meet the recent requirements for energy storage is solid-state batteries (SSBs). This technology uses solid electrodes and a solid-state electrolyte (SE) instead of the liquid-state electrolytes used in current lithium batteries. Although most promising for the future, the diffusion of SSBs must necessarily involve further development of this technology in terms of materials, processing techniques, and cell integration [45]. The use of solid-state electrolytes coupled with lithium anodes allows for reaching higher specific energy and energy densities, up to 300 Wh/kg and 400 Wh/L respectively, in a safer way and with low or nearly no risk of thermal runaway.

Some of the challenges associated with SSBs are related to the low conductivity of solid electrolytes and the presence of internal resistances at the solid-solid interfaces. Another challenge is the chemical instability of the cells with the formation of undesired reactions at the interfaces. The cathode active materials (CAMs) most used and studied for solid-state batteries (SSBs) are the same used in commercial lithium batteries (LIB). Among these, we, therefore, find LCO, NCA, NMC, LMO, LFP, and LNMO (see Section 3.2). LCO turned out to be the best for portable devices given the excellent packing density (~4.3 g/cm^3) and capacity of up to 180 mAh/g. However, reduced structural stability and interface problems prevent their use at high voltages. For this reason, and also due to the high cost of cobalt, NCA- and MNC-type cathodes are a better commercial choice. NCA electrodes yield capacities of ~200 mAh/g in the range of 3.0–4.2 V, while for NMC, especially NMC811 chemistry, capacities up to ~200 mAh/g in the range 3.0–4.3 have been announced. LFP and NMO chemistries instead offer a safer alternative, however, at the expense of lower energy densities. Capacities go up to 170 mAh/g and 120 mAh/g, respectively. LNMO electrodes represent an interesting Co-free high-energy alternative with capacities up to 147 mAh/g [45].

Similarly to what has been said for CAMs, negative electrode materials also derive from those already developed for lithium batteries. Lithium metal is the ideal candidate; in fact, it is characterised by a very low reduction potential (–3.04 V), it is light (0.534 g/cm^3), and it has the highest theoretical capacity (3860 mAh/g). However, some challenges still need to be resolved. In particular, in the formation of lithium dendrites, there is low Culombic efficiency due to the loss of lithium in the solid electrolyte interface (SEI) and cyclability problems. Again, graphite is another widely used anode in lithium batteries, and its use has also been tested in solid-state batteries. The obtainable capacities are around 372 mAh/g. Moreover, pure silica electrodes have been tested, as the maximum theoretical capacities are around 3600 mAh/g. However, volume variations during charge and discharge represent the biggest obstacle to their commercialisation [45].

Regarding solid electrolyte materials, it is possible to distinguish between oxide and polyanionic compounds, sulfides, phospides, and solid polymer electrolytes.

In the first category, we find lithium superionic conductors (LISICONs). These electrolytes have high ionic conductivities at a temperature of 300 °C. Furthermore, they are stable in water, and their low vapour pressure makes them suitable for high-temperature applications. The main disadvantage is their low ionic conductivity at room temperature, although some new chemicals try to mitigate this disadvantage. Still, LISICONs are highly reactive with lithium metal and atmospheric CO_2 [45]. Another type of electrolyte is the so-called sodium superionic conductor (NASICON) with the chemical formula $Na_{1+x}Zr_2Si_xP_{3-x}O_{12}$ $(0 < x < 3)$. In a broader sense, they are also used for similar compounds where Na, Zr, and/or Si are replaced by isovalent elements. Generally, NASICONs are characterised by good ionic conductivity, even at room temperature, resistance to humidity, and good stability range. These types of electrolytes are characterised by high ionic conductivity and high modulus of elasticity; however, the conductivity at room temperature is limited by the oxidation of Ti, which is in contact with metallic lithium. Stability and reduced electronic conductivity make these materials attractive candidates for use as solid electrolytes. However, there are problems with resistance and poor interface contact with lithium metal. Furthermore, stability problems are encountered due to reactivity in the presence of moisture and the formation of Li_2CO_3 at the interface, causing detrimental effects. Finally, one of the most studied solid electrolytes is lithium phosphorous oxynitride (LiPON). This has a conductivity of about 10^{-6} S/cm, which is good chemical stability against lithium and good compatibility with various electrodes [43].

Among sulfides, we can identify glassy sulfides. They are characterised by a low modulus of elasticity but excellent formability even at room temperature. Typical ion conductivity values are in the range of $10^{-3}/10^{-4}$ at room temperature. Crystalline sulfides have a structure similar to LISICONs and appear to be a promising alternative to glassy sulfides. They are characterised by high ionic conductivities even at room temperature. Finally, we have the sulfide-based lithium argyrodite family. The main limitation of sulfides (glassy, glass–ceramic, and/or crystalline) is the reduced electrochemical stability and generation of H_2S in contact with moisture [45].

Lithium phosphides (LiP) are Li superionic conductors that have emerged in recent years. They have promising ionic conductivities; however, research into the stability and compatibility of these electrolytes still needs to be conducted [45].

Solid polymer electrolytes (SPEs) generally consist of ionically conducting solutions of a lithium salt in a polymer host matrix. Polyethylene oxide (PEO) is certainly the most used host matrix in SPEs. PEO at room temperature is characterised by a semicrystalline form and shows ionic conductivities lower than 10^{-5} S/cm, therefore lower than other electrolytes. For this reason, PEO is typically used at operating temperatures of 60 °C or higher [45].

Next, Table 5 shows the basic performance of solid-state batteries taken from the literature [46]. As said, the research has been focused until now on a few demonstrators without large manufacturers capable of moving from demonstrators to commercial products. In Table 5, we see large values of specific energy and specific power: 288 Wh/kg and 3745 W/kg, respectively. However, these numbers are not consolidated among the different types since large variations may occur. Furthermore, ageing data are always rather inadequate. Data about energy densities are even less consolidated. Only for the NCM622 type, another source [47] indicates an energy density of about 400 Wh/L. For the reasons explained, significant growth toward the development of products is expected only by 2030 [48]. Therefore, this technology seems to be significantly far in terms of availability. However, among different state solid batteries, the lithium–sulfur (Li-S) category, which is recalled many times in Table 5, is probably the one with the most likely development and expected commercial diffusion [49].

Table 5. State-solid battery main characteristics.

Solid Electrolyte	"+" Pin Material	"-" Pin Material	Specific Energy (Wh/kg)	Specific Power (W/kg)	Cycles
$Li_{10}SiP_2S_{12}$	NCM111	Li	14	1.8	75
$Li_{10}GeP_2S_{12}$	$LiCoO_2$	Li	20	20	500
$75Li_2S$-$25P_2S_5$	NCA	Li-C	5	1.0	100
$Li_7P_2S_8I$	NCM622	Li	42	34	40
Li_6PS_5Cl	NCM622	Graphite	190	7.9	25
Li_3PS_4 glass	NCM111	Graphite	115	4.0	25
$75Li_2S$–$25P_2S_5$	NCM111	Graphite	155	9.2	30
$Li_{10}GeP_2S_{12}$ & $Li_{9.6}P_3S_{12}$	$LiCoO_2$	Graphite	33	3745.0	25
$Li_{10}GeP_2S_{12}$ & LiI-Li_2S–P_2S_5	$LiCoO_2$	Graphite	180	175.7	25
$80Li_2S$–$20P_2S_5$	NCA	Graphite	39	42.6	25
Li_6PS_5Cl	$LiCoO_2$	Graphite	29	33.9	30
$Li_{6.6}P_{0.4}Ge_{0.6}S_5I$	NCM622	$Li_4Ti_5O_{12}$	27	48.0	60
$Li_{10}GeP_2S_{12}$	Co_9S_8	Li	17	64.9	25
$Li_{10}GeP_2S_{12}$	NiS–CNT	Li	22	28.8	25
PEO–LiTFSI & Al-$Li_{6.75}La_3Zr_{1.75}Ta_{0.25}O_{12}$	$LiFePO_4$	Li	288	7.1	60
$Li_7La_3Zr_2O_{12}$	$LiCoO_2$	Li	141	278.8	50
PEO–LiTFSI	$LiFePO_4$	Li	282	100.3	70
SI–PEO–LiTFSI	$LiFePO_4$	Li	168	91.4	70
SI–PEO–LiTFSI	$LiFePO_4$	Li	120	153.6	80

4. E-Fuels

Power-to-X (PtX) are fuel production pathways in which electricity is converted into various gaseous or liquid fuels, such as e-hydrogen, e-methanol, e-methane, dimethyl ether (E-DME), e-ammonia, or e-diesel. These fuels are also named electrofuels (e-fuel) or power-to-liquid (PtL) and are mentioned in the Annexes of the RED II amendments as alternative options for the decarbonisation of the transport sector [50]. Some of these molecules still contain carbon atoms, thus producing CO_2 when used for energy production. The carbon source for the synthesis of e-fuels has to be carefully analysed to define them really carbon neutral.

The PtX process consists of a change of energy vector: electricity is converted to different molecules that store energy in chemical form (Figure 5). Obviously, this process has an efficiency lower than 1 (defined as the ratio between the lower heating value of the e-fuel produced and electrical energy consumed, see Equation (1)) but converts electrical energy into a different form that could be easily stored compared to electricity.

E-fuel production and use should be carefully assessed because they could have negative impacts on the GHG emissions of the energy system. A fair evaluation cannot ignore the analysis of the whole system's load and generation: Only an excess of electricity (generated by nondispatchable renewable sources) is really CO_2-neutral; in all other moments, electricity brings itself a CO_2-equivalent amount [51].
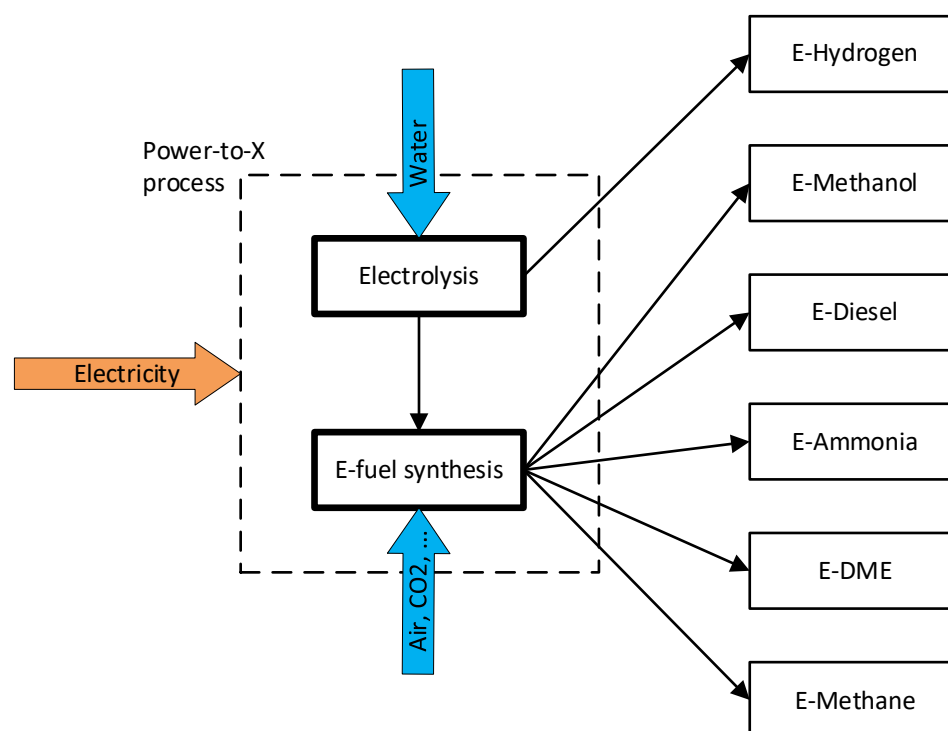
Figure 5. E-fuels production pathways.

Water electrolysis is the fundamental process to convert electrical energy to a chemical one with the production of e-hydrogen, and it is also the first step of all considered PtX pathways.

The e-fuels considered in this paper are reported in Table 6 with their relative mass and energy densities (both gravimetric and volumetric) at 15 °C, 1 atm. The volumetric energy density is a much more relevant limitation for road transport, even more than gravimetric, especially for PCs. There are huge differences between liquid e-fuels and gaseous ones, with up to 3–4 orders of magnitude.

Table 6. E-fuel main properties. Data from [52–54].

	Chemical Formula	LHV [MJ/kg]	LHV [kWh/kg]	Density @15 °C, 1 atm [kg/m³]	LHV @15 °C, 1 atm [kWh/L]	Explosivity Range	Autoignition Temperature [°C]
E-Hydrogen	H_2	120.0	33.3	0.084	0.0028	4–75%	560
E-Methanol	CH_3OH	20.1	5.6	791	4.4164	6–36.5%	420
E-Diesel	C_nH_{2n+2}	43.2	12.0	846	10.1520	1–6%	225
E-Ammonia	NH_3	18.6	5.2	0.72	0.0037	16–25%	630
E-DME	CH_3OCH_3	28.9	8.0	1.96	5.3385	2–50%	350
E-Methane	CH_4	49.9	13.8	0.671	0.0093	5–15%	635

If the comparison is carried out with e-fuels at different conditions, selecting the most viable onboard storage solutions (compressed and liquid E-Hydrogen, compressed and liquid E-Methane, liquid E-Ammonia, liquid E-DME), differences are reduced but still relevant (up to x10, Figure 6). Considering also the containment system for e-fuels, densities are further reduced because cryogenic and high-pressure conditions require tanks with extreme insulation and high mechanical resistance [55]. For example, a cylindric tank containing 4.1 kg of hydrogen at 700 bar has a mass of 66 kg [56] with a huge impact on energy density: from 33.3 kWh/kg of H2 molecule to ca. 2 kWh/kg considering also the tank.
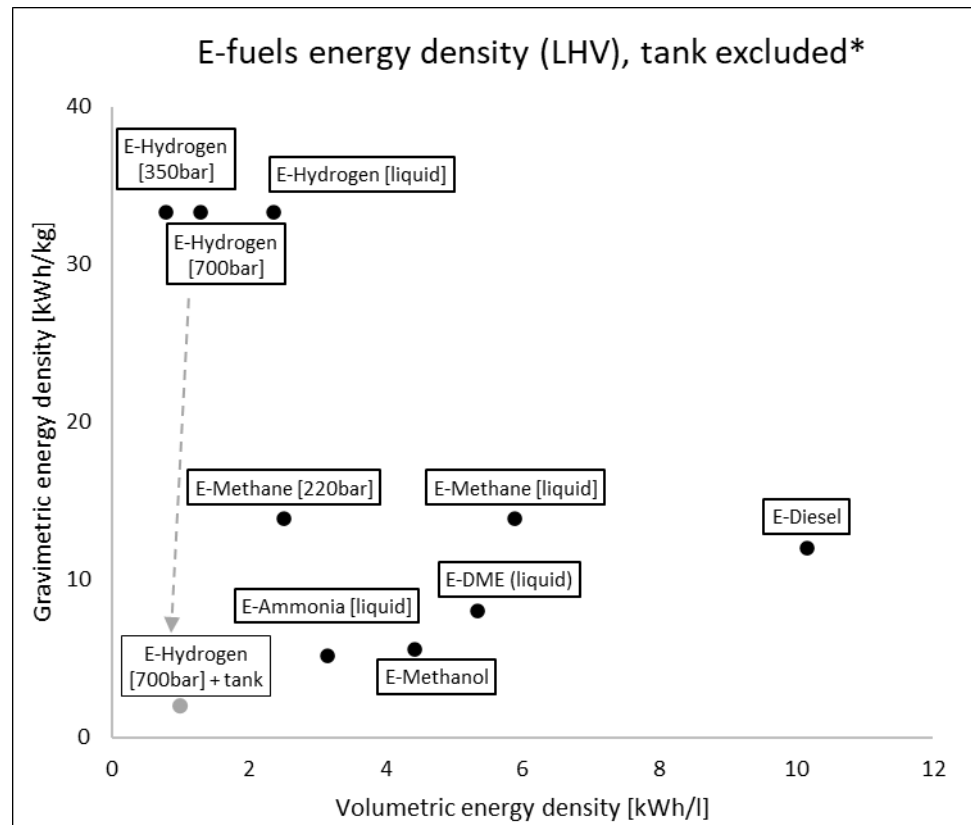
Figure 6. E-fuels gravimetric and volumetric energy density on LHV basis without containing system. * Example of tank influence only for e-hydrogen at 70 MPa.

Moreover, it is important to highlight the amount of energy consumed for compression and liquefaction of e-fuels which must be accounted in a fair 'well-to-wheels' analysis:

- Hydrogen compression to 700bar requires 5.3–6 kWh/kg (16–18% of LHV), liquefaction 10–15 kWh/kg (30–45% of LHV) [53,57,58].
- Methane compression to 220 bar 0.15 kWh/kg (1% of LHV) and liquefaction 0.3–0.6 kWh/kg (2–4% of LHV) [59].

Conversion of e-hydrogen into other e-fuels has a maximum theoretical conversion efficiency (on an LHV basis) determined by the chemical stoichiometry of the synthesis reaction:

$$aH_2 + bR \rightarrow cE + dS \tag{1}$$

where R is the coreactant (CO_2 or N_2), E is the e-fuel, and S is the potential side product. The values of a, b, c, and d depend on the stoichiometry of the reaction. An overall efficiency η_{PtX}, crucial for well-to-wheel analysis, could be defined as the ratio of e-fuel LHV to electrical *PtX*-specific consumption:

$$\eta_{PtX} = \frac{LHV_{e-fuel}}{sc_{PtX}} \tag{2}$$

In Table 7 energetic performance of e-fuel pathways from synthesis to vehicle fuel tank are summarized.

Table 7. E-fuel pathways from synthesis to vehicle tank. Based on [52,59–61].

	Theoretical Conversion Efficiency from Hydrogen	Typical Plant Conversion Efficiency from Hydrogen	Thermophysical Conversion for Storage [kWh/kg]	Typical Overall PtX Efficiency	E-Fuel Transportation to Final User [kWh/kWh$_{fuel}$]	WTT Efficiency
E-Hydrogen (700 bar)	-	-	5.5	0.60	0.09	0.55
E-Hydrogen (liquid)	-	-	11	0.54	0.1	0.49
E-Methanol	0.886	0.797	-	0.53	0.07	0.49
E-Diesel	0.834	0.693	-	0.46	0.05	0.44
E-Ammonia	0.870	0.783	-	0.52	0.07	0.48
E-DME	0.915	0.824	-	0.55	0.07	0.51
E-Methane (220 bar)	0.825	0.743	0.15	0.50	0.07	0.47
E-Methane (liquid)	0.825	0.743	0.5	0.49	0.07	0.46

4.1. E-Hydrogen

E-hydrogen is produced through water electrolysis, an electrochemical process that uses electricity to decompose water into oxygen and hydrogen:

$$H_2O + energy \rightarrow H_2 + \frac{1}{2}O_2 \qquad \Delta H = 285.83 \text{ kJ mol}^{-1} \qquad (3)$$
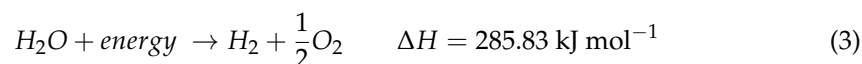
The electrolysers currently available on the market are alkaline electrolysers (AEL); proton exchange membrane electrolysers (PEMEL) are in the development stage, and solid oxide electrolysers (SOEL) are still in the research/demonstration stage [62].

AEL rely on mature and technically well-known technology, and the most used electrolytes are aqueous solutions of potassium hydroxide (KOH) or sodium hydroxide (NaOH). These electrolysers can produce very pure hydrogen and have a relatively low investment cost; however, alkaline electrolytes can be corrosive and cannot start quickly. Instead, in the anode of PEMEL, the water molecule is split into the oxygen, electrons, and protons (H$^+$) passing through the electrolytic membrane, which reach the cathode where they are reduced to form hydrogen molecule H$_2$. PEMEL could also operate with variable load profiles, typical of nonpredictable renewable energy sources (RES), but they need noble metals for electrodes, increasing the capital cost. In SOEL, a flow of water vapour arrives at the cathode where the water is reduced, producing hydrogen molecules and O$_2$-anions which move to the anode where they form an oxygen molecule. SOEL operates at high temperatures, resulting in lower electricity requirements due to thermal activation, but they must be integrated with other heat sources [63]. Table 8 reports the main characteristics of AEL, PEMEL, and SOEL.

Table 8. Main characteristics of electrolyser types. Based on [64–66].

	AEL	PEMEL	SOEL
Temperature range [°C]	60–90	50–90	500–1000
Pressure range [barA]	2–30	15–30	<30
Energy consumption [kWh/kgH$_2$]	50–73	50–73	>42
Lifetime of stack [h]	<90,000	<20,000	<40,000
Lifetime of system [year]	20–30	10–20	-
Capital cost [€/kW]	800–1500	900–2200	<2000
Technology readiness level [TRL]	9	5–7	3–5

So-called 'Green Hydrogen' refers to hydrogen produced by electrolysis using excess electricity generated by renewable sources that cannot be dispatched. 'Yellow Hydrogen',

on the other hand, is produced through electrolysis without relying exclusively on surplus electricity and thus has a CO_2 equivalent emission [51] that must be considered in an accurate well-to-wheels evaluation for its end use, such as for road transport vehicles.

In this paper, the specific electrical consumption of 50 kWh/kgH$_2$ is assumed for electrolysis (LHV-based efficiency of ca. 67%). This value is aligned with the best current electrolyser efficiency of 65% adopted by IRENA [67].

Onboard energy conversion from hydrogen could rely both on ICEs and FCs. Many studies have been carried out in past decades on ICEs fuelled by hydrogen, which is a proper fuel for SI-ICEs due to its high octane number (RON) and easy ignitability. BMW, in the 2000s, revealed a special version of the 760 model with a 12-cylinder, 6-litre direct injection hydrogen engine. Consumption measured in the US highway cycle test was equal to 2.1 kg per 100 km [68]. Other manufacturers, such as Toyota, developed hydrogen ICEs, in particular, for motorsport purposes, and recent tests showed an efficiency of up to 42.6% with very low pollutant emissions [69]. As a whole, from the literature, it can be argued that the efficiency of a hydrogen ICE is slightly lower than the diesel ones currently in operation [70].

Fuel cells (FC) are energy conversion devices that convert the chemical energy of a fuel directly into electrical energy. With respect to thermal machines based on fuel combustion, they have better efficiency and lower noise and pollutant emissions. Different types of FCs can be identified, such as electrolysers, based on the electrolyte used: alkaline (AFCs), proton exchange membrane (PEMFCs), phosphoric acid fuel cells (PAFCs), solid oxide fuel cells (SOFCs), molten carbonate fuel cells (MCFCs) [71]. Hydrogen FCs for road transport are basically PEMFC (Toyota, Honda, and Hyundai existing FCV) due to lower operating temperatures and compactness with respect to other technologies. However, all existing FCVs are also equipped with electrochemical storage because PEMFCs are still unable to provide power profiles with high variability and are unable to recover power from vehicle braking [72].

4.2. E-Methanol

Methanol is currently derived almost entirely from fossil fuels (natural gas for about 85% and coal for about 15%) [73], and it is used for the production of formaldehyde from which plastics and other coating products are obtained. It can be synthesised directly from H_2 and CO_2, usually with copper and zinc-based catalysts, in a reactor usually operating at 230–250 °C and 80 bar. To produce 1 kg of methanol, 1.37 kg of CO_2 and 0.19 kg of H_2 are required.

$$CO_2 + 3H_2 \rightarrow CH_3OH + H_2O \qquad \Delta H = -49.4 \text{ kJ mol}^{-1} \qquad (4)$$

One of the first large-scale conversions of CO_2 to methanol dates back to the first 1990s by Lurgi AG, which developed a two-stage process [74], and since then, dozens of plants were designed and built [75]. In the case of e-methanol, obviously, hydrogen is produced with water electrolysis, and CO_2 is captured directly from the air or from flue gas that eventually would be released in the ambient. In Iceland is operating a plant of e-methanol that use carbon dioxide recovered from geothermal power stations with an overall efficiency of 0.42 [76]. There are several technologies available for CO_2 capture reported in Table 9: Industrial separation and postcombustion are widely used (TRL up to 9) followed by precombustion, oxy-fuel combustion (from TRL up to 7), and DAC (TRL 7) [77].

Table 9. Energetic performance of CO_2 capture technologies. Based on [52,77].

CO₂ Capture Technology	CO₂ Removal Efficiency [%Vol]	Energy Consumption [kWh/kgCO₂]
Industrial Separation	90	1.38
Postcombustion	90	1.15
Precombustion	90	0.93
Oxy-Fuel Combustion	>90	1.13
Direct Air Capture (DAC)	85–93	1.45

Electricity consumption, only for the reactants needed to synthesise 1 kg of e-methanol, is about 10 kWh for H_2 and up to 2 kWh for CO_2 (considering DAC) with a proportion of 5:1. Electrolysis is the most energy-consuming step of the whole process, but carbon dioxide also has a non-negligible impact.

Methanol can be easily used in SI-ICE due to its characteristics: high RON, high heat of vaporisation, high energy per unit of fuel–air mixture, high flame speed, low combustion temperature, and a high hydrogen-to-carbon ratio. Methanol can be burned as a single fuel or blended with gasoline. The modifications needed for spark-ignition ICEs are simple, and a significant amount of gasoline/alcohol flex-fuel ICE is currently running around the world [78].

Regarding FCs, the direct use of methanol is possible (DMFCs), but the technology is only at the research stage [79]. Methanol could be also reformed onboard to hydrogen and used in PEMFCs, but this concept seems limited to bigger applications, such as water transport and not road transport.

4.3. E-Diesel

Historically, the Fischer–Tropsch (FT) process was used to convert syngas (CO/H_2) to liquid hydrocarbons as an alternative route with respect to traditional fossil–oil refineries. FT could not only be coupled to coal gasification and natural gas (NG) reforming but also biomass [80]; the reaction equation, where n is typically 10–20, is:

$$(2n + 1)\,H_2 + nCO \rightarrow C_nH_{2n+2} + H_2O \qquad \Delta H = n(-146)\text{ kJ mol}^{-1} \qquad (5)$$

Direct utilisation of CO_2 and H_2 (from electrolysis) is possible with direct hydrogenation of CO_2 to alkanes [81], but it is still at a very early stage of research [75]. The existing real plants rely on the shift of CO_2 to CO to replicate the syngas composition of traditional coal/NG FT plants [82]. A CO_2 shift could be obtained in a reverse water gas shift (RWGS) reactor or in coelectrolysis as demonstrated by the few projected/existing pilot plants [83,84].

E-diesel production through FT-synthesis, starting from electrolytic H_2, has an efficiency factor of 0.82 to 0.83 [60], which is lower than other e-fuel routes due to the complex upgrading process. On the other hand, e-diesel is the most 'transparent' e-fuel regarding its logistics, refuelling network, and onboard use: E-diesel could be used in existing ICE vehicles and gas stations simply as a substitute or additive to current fossil diesel.

4.4. E-Ammonia

The production of ammonia (NH_3) is carried out by the Haber–Bosch process in which hydrogen, usually produced by the reforming of natural gas, reacts with nitrogen at 400–450 °C and 150–200 bar with an iron catalyst.

$$N_2 + 3H_2 \rightarrow 2NH_3 \qquad \Delta H = -91.8\text{ kJ mol}^{-1} \qquad (6)$$
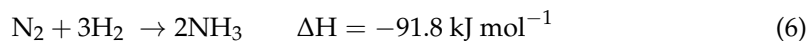
The optimal H_2/N_2 ratio is 2; each step allows for a conversion of about 25–35%. The ammonia is separated from the gas stream before recycling to the reactor, usually by cooling to −25 °C, which causes ammonia liquefaction [85]. To produce 1 kg of e-ammonia, 0.18 kg

of H_2 and 0.82 kg of N_2 are needed. In the case of e-ammonia, obviously, hydrogen will be produced via water electrolysis with the abovementioned technologies (AEL, PEMEL, SOEL). The combination with SOEL has the potential to achieve a better coupling with the ammonia synthesis process with higher efficiencies (up to 0.7 [55]) due to heat integration. However, this technology readiness is very low [86]. The nitrogen needed for the Haber–Bosch process is captured from ambient air with three possible technologies: cryogenic separation, pressure swing adsorption (PSA), and membrane permeation. For large-scale ammonia plants, cryogenic distillation is the more convenient option due to the lowest specific consumption which is equal to 0.11 kWh/kgN_2 [87,88].

Electricity consumption, only for the reactants needed to synthesise 1 kg of e-ammonia, is about 9 kWh for H_2 and 0.09 kWh for N_2 (considering cryogenic separation) with a proportion of 100:1. So, nitrogen separation consumption has a minimal impact on overall e-ammonia production, which reaches global efficiencies above 0.5 in existing large-scale plants [85].

Regarding application in ICEs, ammonia has significantly higher ignition energy and lower flammability when compared with fossil fuels. However, many ICE applications were conceived and tested in the last century [89], both spark and compression ignited [90]. Ammonia could also be burned in ICEs with a combustion promoter such as hydrogen, which can be obtained directly by onboard reforming a small portion of ammonia itself [91].

With onboard reforming and purification, hydrogen PEMFCs can also be used, but the cost and dimension of the whole system are unsuitable for road transport. Direct use of ammonia in FCs is possible, in particular, with alkaline electrolyte types and solid electrolyte types. High-temperature ceramic fuel cells are the most promising because the high operating temperature (>600 °C) could promote ammonia decomposition with the presence of catalysts [92]. However, these technologies have volume and mass requirements that are not compatible with road transport.

4.5. E-DME

Historically DME was a by-product of high-pressure methanol synthesis, but nowadays, it is produced exclusively by methanol dehydration in a so-called 'two-stage synthesis'. However, DME can also be synthesised directly from syngas, such as e-diesel in FT processes, with two viable reaction routes:

$$3CO + 3H_2 \rightarrow CH_3OCH_3 + CO_2 \qquad \Delta H = -246 \text{ kJ mol}^{-1} \qquad (7)$$

$$2CO + 4H_2 \rightarrow CH_3OCH_3 + H_2O \qquad \Delta H = -205 \text{ kJ mol}^{-1} \qquad (8)$$
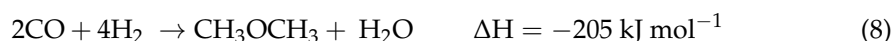
Both reactions are used in commercial plants [75]. For E-DME, besides electrolytic hydrogen, the carbon source is CO_2, which can be easily converted into CO with an RWGS. Direct hydrogenation of CO_2 to DME has been investigated [93], but it is still at a low level of technological readiness [94].

DME has a high cetane number, low ignition temperature, and high speed of vaporisation when injected into the cylinder. These characteristics make it a suitable fuel for CI-ICEs, with almost smoke-free combustion [95], while the low RON makes application in SI-ICEs difficult. High exhaust gas recirculation (EGR) rates can be used to reduce NOx without penalties for PM and HC emissions. On the other hand, DME CI-ICEs emit more CO than diesel. [96].

Only a few studies of direct DME-FCs can be found in the literature [97,98], while the use of PEMFC with an onboard reformer has gained attention in recent years [99]. However, both solutions seem inapplicable to road transport because of high temperature and volume/mass requirements.

4.6. E-Methane

Methane is the main component of fossil natural gas, and this is the main source of methane besides non-negligible biologic production, mainly from the anaerobic digestion of biomasses. However, methane could be synthesised with the hydrogenation of CO_2:

$$CO_2 + 4H_2 \rightarrow CH_4 + 2H_2O \qquad \Delta H = -165 \text{ kJ mol}^{-1} \tag{9}$$

E-methane, often called also synthetic natural gas (SNG), is produced with this reaction, also called the 'Sabatier reaction' in honour of the French chemist Paul Sabatier who discovered it. Usually, the CO_2 is compressed up to 30 bar and introduced into a methanation reactor at 300 °C [59]. These are the optimal operating conditions for the Sabatier reaction to occur [100].

Methane use in ICEs is a well-known application with fossil natural gas, especially in SI. Many PCs from different manufacturers are currently available on the market and equipped with tanks for compressed NG. The cryogenic liquid form (LNG) is also an attractive energy vector for heavy-duty trucks with much lower emissions than diesel and biomethane and bio-LNG cases proving the feasibility of decentralised production [101].

5. Discussion

The decarbonisation of electricity generation represents unprecedented support for the decarbonisation of road transport stuck to fossil fuels until now. This opportunity, along with technological improvement of onboard energy storages and electric drives, will forever change road vehicles and their primary energy source. PCs and LCVs are the first categories affected by this paradigm shift, while HDTs will be right behind.

Additionally, e-fuels represent an interesting possibility to easily store decarbonised electricity in a different form, turning it into chemical energy. Nowadays, e-fuels face three main issues: energy density, production pathways, and onboard conversion.

- Regarding volumetric energy density, e-hydrogen is the most difficult e-fuel to store onboard due to its lower density even at extreme cryogenic conditions. Compressed hydrogen requires tanks with a remarkable mass, drastically reducing the gravimetric energy density (from 33.3 kWh/kg to 2 kWh/kg, Figure 6). E-methane seems more feasible looking at existing vehicles fuelled with fossil natural gas (compressed for PCs and LCVs, liquid for HDTs). Other liquid e-fuels are more easily storable onboard, albeit with differences among them and for safety/hazard reasons. E-diesel showed the best energy density and substitutability with current fossil fuels.
- Almost all e-fuel pathways rely on water electrolysis to produce hydrogen (the simplest e-fuel) and then on its conversion to other molecules using CO_2 or N_2 as side reactants. Water electrolysis, particularly with AEL, is a market-ready technology, while plants for hydrogen conversion to other chemicals are still immature with only a few pilot plants. However, a huge carry-over from existing synthesis technology of the same molecules is possible, especially for methanol and ammonia. All e-fuel pathways, from input electricity to vehicle tanks, are energy-consuming processes with efficiency ranging between 0.44–0.55.
- Onboard use of e-fuel is possible both with ICEs and FCs. The internal combustion engine is a well-known device deeply developed in the last century, and many studies have been carried out with all considered e-fuels proving at least their feasibility. Hydrogen fuel cells reached a decent technology maturity with PEMFC, but many improvements are still possible. Instead, other FCs for direct use of different e-fuels are much more immature or not suitable for road transport (high-temperature FCs). It is important to remember that other pollutants (CO, NOx, PM, NH_3, ...) may be locally emitted with e-fuels, especially if burned in ICEs.

A brief comparison of BEV and e-fuels has been carried out considering 15 kWh/100 km of energy consumed (energy to the wheels) for a medium-sized PC in the Worldwide Harmonised Light Vehicles Test Procedure (WLTP). This value stands between 12.4 kWh/100 km

(post-2025 BEV WLTP simulated by JEC [7]) and 16.6 kWh/km (WLTP homologation average of new BEV registrations in 2021 in EU [11]). In all the considered cases, a BEV based on standard lithium-based technology has been considered.

Looking at the real fuel consumption of current Italian ICE-PCs in Table 1 (63.6 and 65.6 kWhfuel/100 km), a current average efficiency TTW could be calculated as ca. 0.25. However, a higher value, 0.35, was selected (corresponding to ca. 4.5 L/100 km of gasoline), considering that future ICE HEV-PCs will use only hybrid powertrains with a better overall TTW efficiency than the current ones. Regarding FC-HEVs, an efficiency equal to 0.5 has been selected, considering the onboard energy conversion of e-fuel into effective vehicle propulsion (FC, DC/DC conversion, inverter, electric motor).

Regarding BEVs, an overall current WTW efficiency of 0.77 taken from [102] has been considered (0.81 in 2050 [103]). In consideration of the current status of technology for electric drive and storage, it is possible to consider an average value of about 0.90 for the TTW part. For BEVs, only one storage system typology (e.g., lithium-based battery) was considered in Table 10. In fact, by moving towards other technologies beyond lithium, no significant changes regarding specific energy and efficiency have been observed; therefore, it can be concluded that there will be no significant changes in the evaluation of corresponding energy consumption and WTW efficiency. On the other hand, significant transformations, with corresponding modifications for the consumed energy, will mainly affect processes related to the construction and dismantling of new generations of storage due to the utilisation of different materials. However, these contributions are out of the present analysis, and therefore will not be shown.

Table 10. Energetic comparison of e-fuels and batteries in medium-sized PCs.

Powertrain Type	ENERGY VECTOR	WTT Efficiency	TTW Efficiency	WTW Efficiency	Specific Electricity Consumption for Medium-Sized PCs in WLTP [kWh/100 km]
BEV	Electricity	0.85	0.90	0.77	19.5
ICE-HEV (plug-in excluded)	E-Hydrogen 700 bar	0.55	0.35	0.19	78.5
	E-Hydrogen (liquid)	0.49	0.35	0.17	88.2
	E-Methanol	0.49	0.35	0.17	86.9
	E-Diesel	0.44	0.35	0.15	98.1
	E-Ammonia	0.48	0.35	0.17	88.6
	E-DME	0.51	0.35	0.18	83.8
	E-Methane 220 bar	0.47	0.35	0.16	92.2
	E-Methane liquid	0.46	0.35	0.16	94.0
FC-HEV	E-Hydrogen 700 bar	0.55	0.5	0.27	54.9
	E-Hydrogen (liquid)	0.49	0.5	0.24	61.7
	E-Methanol	0.49	0.5	0.25	60.9
	E-Ammonia	0.48	0.5	0.24	62.0

Table 10 reports the WTT efficiencies previously analysed and the average TTW leading to WTW and specific electricity vehicle WLTP consumption in kWh/100 km.

Normalising specific electricity consumption with respect to BEVs (Figure 7), it is even more evident that e-fuels require 3–5 times more electricity to satisfy the same purpose. This huge gap in efficiency is a crucial difference between electricity and e-fuels because, on the large scale of national/global road transport, such larger electricity demand could represent an insuperable barrier: Renewables capacity and new installation simply may not be able to cope with this additional demand. This paper does not deal with economic implications, but it is self-evident that energy affects the total cost of ownership (TCO) of vehicles: Less efficiency implies a higher operational cost.
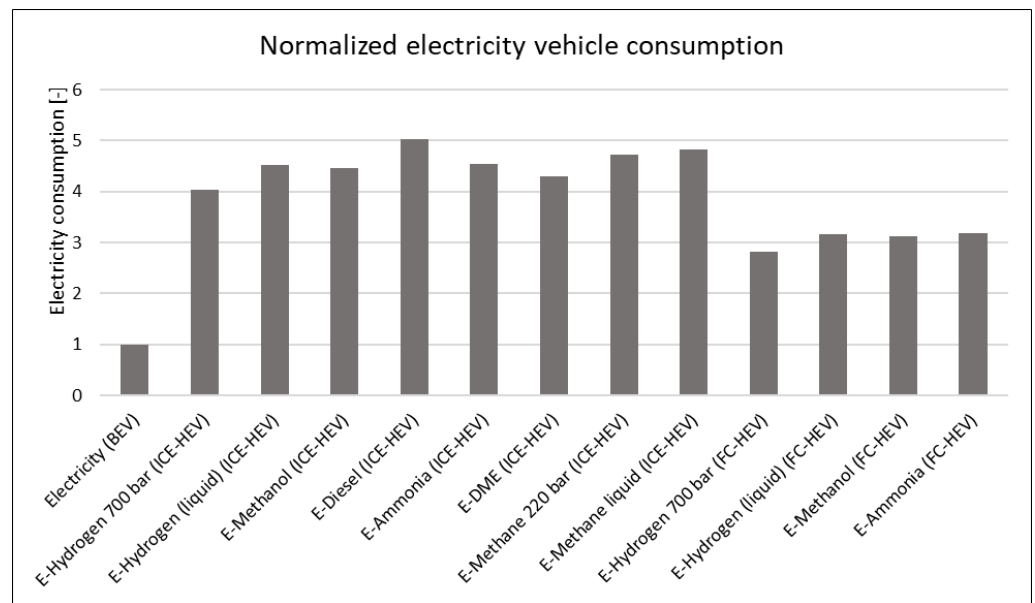
Figure 7. Normalised electricity consumption for average PC with respect to BEV.

If we consider that grid electricity may carry a residual CO_2-specific emission factor, especially during the next decades of transition, then less efficiency also means higher equivalent emissions. In Figure 8, equivalent vehicle emissions in gCO_2/km are plotted versus the electricity emission factor: Solid lines represent powertrains and e-fuels currently 'market ready', while dashed lines indicate lower technology readiness. Electricity used in BEVs has the lowest CO_2 emission in any case, but it is important to note that e-fuels may cause emissions higher than current fossil fuels if electricity is not sufficiently decarbonised.
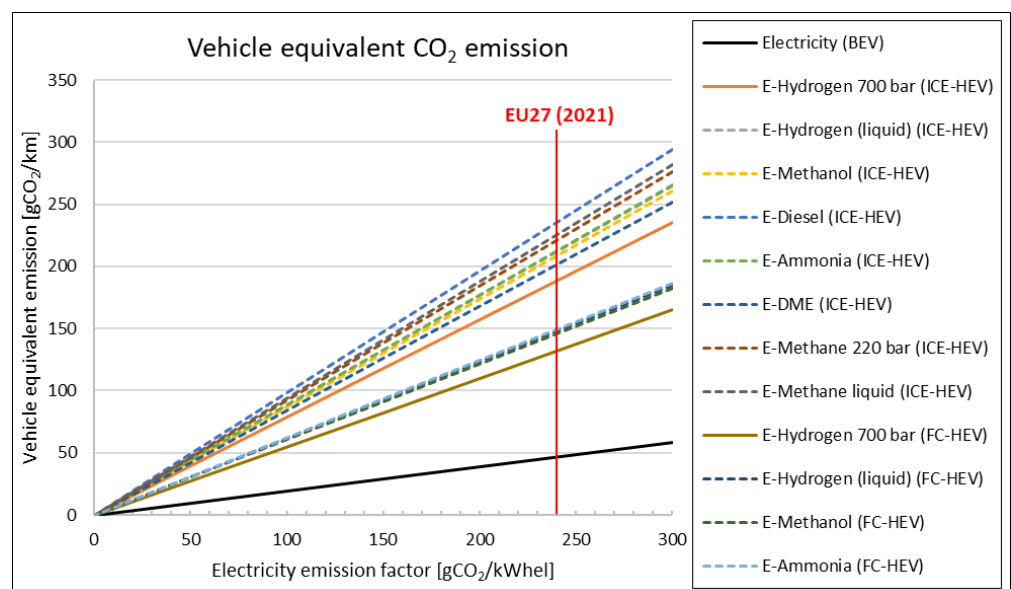
Figure 8. Equivalent CO_2 vehicle emission vs. electricity emission factor.

The emissions intensity of EU27 electricity generation (the amount of GHG emitted per unit of electricity) in the last decades declined to 241 $gCO_2/kWhel$ (the year 2021), even if there are still huge differences among countries (maximum 736 g in Poland and minimum 58 g in France) [104]. With the current EU27 emission factor, PC-BEVs emit less than 50 gCO_2/km, while e-fuels options would range from 140–240 gCO_2/km (higher than current fossil fuel ICE-PCs).

Nomenclature

AEL	Alkaline Electrolyser
BEV	Battery Electric Vehicle
C-HEV	Complex Hybrid Electric Vehicle
CI	Compression Ignition
CNG	Compressed Natural Gas
DAC	Direct Air Capture
DME	Dimethyl Ether
DMFC	Direct Methanol Fuel Cell
EGR	Exhaust Gas Recirculation
FC-HEV	Fuel Cell Electric Vehicle
FCV	Fuel Cell Vehicle
FCS	Fuel Cell System
FT	Fischer–Tropsch
GHG	Greenhouse Gases
HDT	Heavy-duty Truck
HEV	Hybrid Electric Vehicle
LCV	Light Commercial Vehicle
LHV	Lower Heating Value
LPG	Liquefied Petroleum Gas
NG	Natural Gas
PC	Passenger Car
PEMEL	Proton Exchange Membrane Electrolyser
P-HEV	Parallel Hybrid Electric Vehicle
PHEV	Plug-in Hybrid Electric Vehicle
PM	Particulate Matter
PtL	Power to Liquid
PtX	Power to X
RESS	Rechargeable Energy Storage System
RON	Research Octane Number
RWGS	Reverse Water Gas Shift
S-HEV	Series Hybrid Electric Vehicle
SI	Spark Ignition
SNG	Synthetic Natural Gas
SOEL	Solid Oxide Electrolyser
TCO	Total Cost of Ownership
TRL	Technology Readiness Level
TTW	Tank-to-Wheels
WLTP	Worldwide Harmonised Light Vehicles Test Procedure
WTT	Well-to-Tank
WTW	Well-to-Wheels

References

1. United Nations. Day of 8 Billion. Available online: https://www.un.org/en/dayof8billion (accessed on 2 December 2022).
2. United Nations. Climate Action COP27. Available online: https://www.un.org/en/climatechange/cop27 (accessed on 2 December 2022).

3. United Nations Climate Change. Paris Agreement at COP21. Available online: https://unfccc.int/process-and-meetings/the-paris-agreement/the-paris-agreement (accessed on 2 December 2022).
4. DNV. Energy Transition Outlook 2022. 2022. Available online: https://www.dnv.com/Publications/energy-transition-outlook-2022-232649 (accessed on 2 December 2022).
5. Eurostat. European Statistical Dashboard. 2022. Available online: https://ec.europa.eu/eurostat/data/database (accessed on 2 December 2022).
6. Istituto Superiore per la Protezione e la Ricerca Ambientale. National Inventory Report 2021. In *Italian Greenhouse Gas Inventory 1990–2019*; ISPRA: Bologna, Italy, 2021; Rapporti 341/21; ISBN 978-88-448-1046-7.
7. JEC Tank-To-Wheels Report v5. Available online: https://publications.jrc.ec.europa.eu/repository/handle/JRC117560 (accessed on 2 December 2022).
8. World Resources Institute. World Greenhouse Gas Emissions in 2018 (Sector End Use | Gas). 2021. Available online: https://www.wri.org/data/world-greenhouse-gas-emissions-2018 (accessed on 2 December 2022).
9. IEA. Transport Sector CO2 Emissions by Mode in the Sustainable Development Scenario, 2000–2030, IEA, Paris. Available online: https://www.iea.org/data-and-statistics/charts/transport-sector-co2-emissions-by-mode-in-the-sustainable-development-scenario-2000-2030 (accessed on 1 February 2023).
10. European Automobile Manufacturers' Association. *Vehicles in Use in Europe 2022*; ACEA: Brussels, Belgium, 2022.
11. European Environment Agency. New Registrations of Electric Vehicles in Europe, EEA. 2022. Available online: https://www.eea.europa.eu/ims/new-registrations-of-electric-vehicles (accessed on 2 December 2022).
12. European Union. Regulation 2021/1119 of the European Parliament and of the Council of 30 June 2021; 2021. Available online: https://eur-lex.europa.eu/legal-content/EN/TXT/HTML/?uri=CELEX:32021R1119&from=EN (accessed on 1 February 2023).
13. Fit for 55. Available online: https://www.consilium.europa.eu/en/policies/green-deal/eu-plan-for-a-green-transition (accessed on 2 December 2022).
14. European Commission—Press Release. Proposal for a Regulation on Type-Approval of Motor Vehicles with Respect to Their Emissions and Battery Durability (Euro 7); Brussels, 10 November 2022. Available online: https://eur-lex.europa.eu/legal-content/EN/TXT/HTML/?uri=CELEX:52022PC0586&from=EN (accessed on 1 February 2023).
15. Sun, C.; Zhang, H. Review of the development of first-generation redox flow batteries: Iron-chromium system. *ChemSusChem* **2021**, *15*, e202101798. [CrossRef] [PubMed]
16. ISO/TR 8713; Electrically Propelled Road Vehicles—Vocabulary. Available online: https://www.iso.org/home.html (accessed on 2 December 2022).
17. Wang, Y.; Moura, S.J.; Advani, S.G.; Prasad, A.K. Power management system for a fuel cell/battery hybrid vehicle incorporating fuel cell and battery degradation. *Int. J. Hydrog. Energy* **2019**, *44*, 8479–8492. [CrossRef]
18. IEA. *Global EV Outlook 2022*; IEA: Paris, France, 2022.
19. Samsung Cylindrical LCO Cell Datasheet. Available online: https://docs-emea.rs-online.com/webdocs/15d2/0900766b815d2388.pdf (accessed on 1 February 2023).
20. E-one Moli Energy Cylindrical LCO Cell Datasheet. Available online: http://www.molicel.com/wp-content/uploads/DM_ICR18650M-V3-80072.pdf (accessed on 1 February 2023).
21. Envision AESC LMO Cell Datasheet. Available online: https://pushevs.com/2017/09/08/lg-chem-will-introduce-ncm-811-battery-cells-evs-next-year/ (accessed on 1 February 2023).
22. GS Yuasa LMO Battery Datasheet. Available online: http://www.gsyuasa-lp.com/SpecSheets/LIM50EN_Data_Sheet.pdf (accessed on 1 February 2023).
23. Kokam Official Site, High Power Pouch NMC Cell. Available online: http://kokam.com/wp-content/uploads/2016/03/SLPB-Cell-Brochure.pdf (accessed on 1 February 2023).
24. Kokam Official Site, High Energy Pouch NMC Cell. Available online: https://kokam.com/uploaded/filebox/7/cell_brochure.pdf (accessed on 1 February 2023).
25. LG Cylindrical NMC Cell Datasheet. Available online: https://cdn.shopify.com/s/files/1/0674/3651/files/lg-hg2-spec-sheet.pdf (accessed on 1 February 2023).
26. Samsung Cylindrical NMC Cell Datasheet. Available online: https://docs.rs-online.com/84c8/0900766b812fdd47.pdf (accessed on 1 February 2023).
27. Samsung Prismatic NMC Cell Datasheet. Available online: https://files.gwl.eu/inc/_doc/attach/StoItem/7213/30118_Introduction%20of%20SDI%20EV%2094Ah%20cell_V9-2.pdf (accessed on 1 February 2023).
28. Panasonic Cylindrical NCM 21700. Available online: https://www.batemo.de/products/batemo-cell-library/panasonic-tesla-model-3/ (accessed on 1 February 2023).
29. Panasonic Official Site, High Energy Prismatic NCA Cell. Available online: https://industrial.panasonic.com/ww/products/batteries/secondary-batteries/lithium-ion/prismatic-type/NCA103450 (accessed on 1 February 2023).
30. Samsung Official Site, NCA Cell. Available online: https://www.powerstream.com/p/INR18650-25R-datasheet.pdf (accessed on 1 February 2023).
31. Winston Official Site, Prismatic LFP Cell. Available online: http://en.winston-battery.com/index.php/products/power-battery/category/lithium-ion-power-battery (accessed on 1 February 2023).

32. A123 Nanophosphate High Power Cylindrical LFP Cell Datasheet. Available online: https://www.batteryspace.com/prod-specs/6610.pdf (accessed on 1 February 2023).
33. GWL Prismatic LFP Datasheet. Available online: https://files.gwl.eu/inc/_doc/attach/StoItem/4091/ZG-LFP060AHA_datasheet.pdf (accessed on 1 February 2023).
34. CATL Prismatic LFP Datasheet. Available online: https://www.lifepo4-battery.com/Products/CATL-Battery/CATL-161Ah-battery.html (accessed on 1 February 2023).
35. Toshiba Official Site, High Power Prismatic LTO Cell. Available online: https://www.scib.jp/en/product/cell.htm (accessed on 1 February 2023).
36. GWL Cylindrical LTO Cell Datasheet. Available online: https://files.ev-power.eu/inc/_doc/attach/StoItem/7015/GWL_LTO1865_Rechargeable.pdf (accessed on 1 February 2023).
37. Olabi, A.G.; Sayed, E.T.; Wilberforce, T.; Jamal, A.; Alami, A.H.; Elsaid, K.; Rahman, S.M.A.; Shah, S.K.; Abdelkareem, M.A. Metal-Air Batteries—A Review. *Energies* **2021**, *14*, 7373. [CrossRef]
38. Gelman, D.; Shartsev, B.; Ein-Eli, Y. Aluminum-Air Battery Based on an Ionic Liquid Electrolyte. *J. Mater. Chem.* **2014**, *2*, 20237–20242. [CrossRef]
39. Weinrich, H.; Durmus, Y.E.; Tempel, H.; Kungl, H.; Eichel, R.A. Silicon and Iron as Resource-Efficient Anode. *Materials* **2019**, *12*, 2134. [CrossRef] [PubMed]
40. Montanino, M.; Prosolini, P.P. *Batterie Metallo Aria: Stato Dell'arte e Prospettive*; ENEA: Rome, Italy, 2013.
41. Great River Energy Official Site. Available online: https://greatriverenergy.com/company-news/battery-project-includes-minnesota-flair/ (accessed on 1 February 2023).
42. Wang, C.; Yu, Y.; Niu, J.; Liu, Y.; Bridges, D.; Liu, X.; Pooran, J.; Zhang, Y.; Hu, A. Recent Progress of Metal–Air Batteries—A Mini Review. *Appl. Sci.* **2019**, *9*, 2787. [CrossRef]
43. CATL Official Site. Available online: https://www.catl.com/en/news/665.html (accessed on 9 December 2022).
44. He, M.; Davis, R.; Chartouni, D.; Johnson, M.; Abplanalp, M.; Troendle, P.; Suetterlin, R.P. Assessment of the first commercial Prussian blue based sodium-ion battery. *J. Power Sources* **2022**, *548*, 232036. [CrossRef]
45. Boaretto, N.; Garbayo, I.; Valiyaveettil-SobhanRaj, S.; Quintela, A.; Li, C.; Casas-Cabanas, M.; Aguesse, F. Lithium solid-state batteries: State-of-the-art and challenges for materials. *J. Power Sources* **2021**, *502*, 229919. [CrossRef]
46. Randau, S.; Weber, D.A.; Kötz, O.; Koerver, R.; Braun, P.; Weber, A.; Ivers-Tiffée, E.; Adermann, T.; Kulisch, J.; Zeier, W.G.; et al. Benchmarking the performance of all-solid-state. *Nat. Energy* **2020**, *5*, 259–270. [CrossRef]
47. Nam, Y.J.; Oh, D.Y.; Jung, S.H.; Jung, Y.S. Toward practical all-solid-state lithium-ion batteries with high energy density and safety: Comparative study for electrodes fabricated by dry- and slurry-mixing processes. *J. Power Sources* **2018**, *375*, 93–101. [CrossRef]
48. Saurabh, D.; Yerukola, P. *Solid State Battery Market Report*; 2022; p. 230; report code: A00398. Available online: https://www.alliedmarketresearch.com/solid-state-batteries-market (accessed on 1 February 2023).
49. Bandyopadhyay, S.; Nandan, B. A review on design of cathode, anode and solid electrolyte for true all-solid-state lithium sulfur batteries. *Mater. Today Energy* **2023**, *31*, 101201. [CrossRef]
50. European Union. *Directive 2018/2001 of the European Parliament and of the Council of 11 December 2018 on the Promotion of the Use of Energy from Renewable Sources*; Official Journal of the European Union, 21 December 2018. Available online: https://eur-lex.europa.eu/legal-content/EN/TXT/HTML/?uri=CELEX:32018L2001&from=EN (accessed on 1 February 2023).
51. Liponi, A.; Pasini, G.; Baccioli, A.; Ferrari, L. Hydrogen from renewables: Is it always green? The Italian scenario. *Energy Convers. Manag.* **2023**, *276*, 116525. [CrossRef]
52. Tremel, A. *Electricity-Based Fuels*; Springer International Publishing: Cham, Switzerland, 2018; pp. 39–41.
53. Sundén, B. (Ed.) Hydrogen, Batteries and Fuel Cells. In *Chapter 3-Hydrogen*; Academic Press: New York, NY, USA, 2019; pp. 37–55.
54. NOAA. CAMEO Chemicals Version 2.8.0 rev 1. Available online: https://cameochemicals.noaa.gov/ (accessed on 1 February 2023).
55. DNV. *White Paper: Ammonia as a Marine Fuel*; DNV GL—Group Technology & Research 2020. Available online: https://www.dnv.com/Publications/ammonia-as-a-marine-fuel-191385 (accessed on 1 February 2023).
56. Hyundai NEXO Tank Supplier. Available online: https://hyfindr.com/marketplace/components/hydrogen-tanks/hydrogen-type-4-cylinder-700-bar-103l/ (accessed on 9 December 2022).
57. Sheeld, J.; Martin, K.; Folkson, R. Alternative Fuels and Advanced Vehicle Technologies for Improved Environmental Performance. In *5-Electricity and Hydrogen as Energy Vectors for Transportation Vehicles*; Folkson, R., Ed.; Woodhead Publishing: Cambridge, UK, 2014; pp. 117–137.
58. Kim, H.; Haider, J.; Qyyum, M.A.; Lim, H. Mixed refrigerant–based simplified hydrogen liquefaction process: Energy, Exergy, economic, and environmental analysis. *J. Clean. Prod.* **2022**, *367*, 132947. [CrossRef]
59. Baccioli, A.; Bargiacchi, E.; Barsali, S.; Ciambellotti, A.; Fioriti, D.; Giglioli, R.; Pasini, G. Cost effective power-to-X plant using carbon dioxide from a geothermal plant to increase renewable energy penetration. *Energy Convers. Manag.* **2020**, *226*, 113494. [CrossRef]
60. Hannula, I.; Kurkela, E. *Liquid Transportation Fuels Via Large-Scale Fluidised-Bed Gasification of Lignocellulosic Biomass*; VTT Technical Research Centre of Finland: Espoo, Finland, 2013.

61. Prussi, M.; Yugo, M.; Padella, M.; Edwards, R.; Lonza, L.; De Prada, L. *JEC Well-to-Tank Report v5: Annexes*; Hamje, H., Ed.; EUR 30269 EN; Publications Office of the European Union: Luxembourg, 2020; ISBN 978-92-76-21707-7. [CrossRef]

62. Shiva Kumar, S.; Lim, H. An overview of water electrolysis technologies for Green Hydrogen production. *Energy Rep.* **2022**, *8*, 13793–13813. [CrossRef]

63. Buttler, A.; Spliethoff, H. Current status of water electrolysis for energy storage, grid balancing and sector coupling via power-to-gas and power-to-liquids: A Review. *Renew. Sustain. Energy Rev.* **2018**, *82*, 2440–2454. [CrossRef]

64. Sebbahi, S.; Nabil, N.; Alaoui-Belghiti, A.; Laasri, S.; Rachidi, S.; Hajjaji, A. Assessment of the three most developed water electrolysis technologies: Alkaline water electrolysis, proton exchange membrane and solid-oxide electrolysis. *Mater. Today Proc.* **2022**, *66*, 140–145. [CrossRef]

65. Bos, M.J.; Kersten, S.R.A.; Brilman, D.W.F. Wind power to methanol: Renewable methanol production using electricity, electrolysis of water and CO_2 Air Capture. *Appl. Energy* **2020**, *264*, 114672. [CrossRef]

66. MCPHY Technical Specification. Available online: https://mcphy.com/en/equipment-services/electrolyzers/ (accessed on 1 February 2023).

67. IRENA. Green Hydrogen Cost Reduction: Scaling up Electrolysers to Meet the 1.5 °C Cimate Goal, Abu Dhabi. 2020. Available online: https://www.irena.org/publications/2020/Dec/Green-hydrogen-cost-reduction (accessed on 1 February 2023).

68. Wallner, T.; Lohse-Busch, H.; Gurski, S.; Duoba, M.; Thiel, W.; Martin, D.; Korn, T. Fuel economy and emissions evaluation of bmw hydrogen 7 mono-fuel demonstration vehicles. *Int. J. Hydrog. Energy* **2008**, *33*, 7607–7618. [CrossRef]

69. Bao, L.-Z.; Sun, B.-G.; Luo, Q.-H.; Li, J.-C.; Qian, D.-C.; Ma, H.-Y.; Guo, Y.-J. Development of a turbocharged direct-injection hydrogen engine to achieve clean, efficient, and high-power performance. *Fuel* **2022**, *324*, 124713. [CrossRef]

70. DNV. *Assessment of Selected Alternative Fuels and Technologies*; DNV GL—Group Technology & Research. 2019. Available online: https://www.dnv.com/maritime/publications/alternative-fuel-assessment-download.html (accessed on 1 February 2023).

71. Fan, L.; Tu, Z.; Chan, S.H. Recent development of hydrogen and Fuel Cell Technologies: A Review. *Energy Rep.* **2021**, *7*, 8421–8446. [CrossRef]

72. Gherairi, S. Hybrid Electric Vehicle: Design and control of a hybrid system (fuel cell/battery/ultra-capacitor) supplied by Hydrogen. *Energies* **2019**, *12*, 1272. [CrossRef]

73. IHS Chemicals. *Global Methanol Weekly Report 23 March 2012, IHS Chemical Market Advisory Service Issue (2012)*; IHS Chemicals: London, UK, 2012; p. 1509.

74. Goehna, H.; Konig, P. Producing methanol from CO_2. *Chemtech* **1994**, *24*, 36–39.

75. Dieterich, V.; Buttler, A.; Hanel, A.; Spliethoff, H.; Fendt, S. Power-to-liquid via synthesis of methanol, DME or Fischer–Tropsch-fuels: A Review. *Energy Environ. Sci.* **2020**, *13*, 3207–3252. [CrossRef]

76. Kauw, M.; Benders, R.M.J.; Visser, C. Green methanol from hydrogen and carbon dioxide using geothermal energy and/or hydropower in Iceland or excess renewable electricity in Germany. *Energy* **2015**, *90*, 208–217. [CrossRef]

77. Hong, W.Y. A techno-economic review on carbon capture, utilisation and storage systems for achieving a net-zero CO2 emissions future. *Carbon Capture Sci. Technol.* **2022**, *3*, 100044. [CrossRef]

78. Verhelst, S.; Turner, J.W.G.; Sileghem, L.; Vancoillie, J. Methanol as a fuel for internal combustion engines. *Prog. Energy Combust. Sci.* **2019**, *70*, 43–88. [CrossRef]

79. Ramli, Z.A.; Shaari, N.; Saharuddin, T.S. Progress and major barriers of nanocatalyst development in direct methanol fuel cell: A Review. *Int. J. Hydrog. Energy* **2022**, *47*, 22114–22146. [CrossRef]

80. EBTP-SABS, Biomass to Liquids (BtL). 2016. Available online: http://www.biofuelstp.eu/btl.html (accessed on 1 February 2023).

81. Riedel, T.; Schaub, G.; Jun, K.-W.; Lee, K.-W. Kinetics of CO_2 Hydrogenation on a K-Promoted Fe Catalyst. *Ind. Eng. Chem. Res.* **2001**, *40*, 1355–1363. [CrossRef]

82. Zhang, C.; Jun, K.-W.; Ha, K.-S.; Lee, Y.-J.; Kang, S.C. Efficient utilization of greenhouse gases in a gas-to-liquids process combined with CO2/steam-mixed reforming and Fe-based Fischer-Tropsch synthesis. *Environ. Sci. Technol.* **2014**, *48*, 8251–8257. [CrossRef]

83. Nordic Electro Fuel—Produce Sustainable Aviation Fuel. Available online: https://nordicelectrofuel.no/ (accessed on 1 February 2023).

84. Sunfire-Synlink Factsheet. Available online: https://www.sunfire.de/files/sunfire/images/content/Produkte_Technologie/factsheets/Sunfire-SynLink_FactSheet.pdf (accessed on 1 February 2023).

85. Rouwenhorst, K.H.R.; Van der Ham, A.G.J.; Mul, G.; Kersten, S.R.A. Islanded Ammonia Power Systems: Technology Review & Conceptual Process Design. *Renew. Sustain. Energy Rev.* **2019**, *114*, 109339. [CrossRef]

86. Zhang, H.; Wang, L.; Van herle, J.; Maréchal, F.; Desideri, U. Techno-economic comparison of green ammonia production processes. *Appl. Energy* **2020**, *259*, 114135. [CrossRef]

87. Thomas, L. Hardenburger, Matthew Ennis. In *Nitrogen*; John Wiley & Sons, Ltd: London, UK, 2005.

88. Sánchez, A.; Martín, M. Scale up and scale down issues of renewable ammonia plants: Towards modular design. *Sustain. Prod. Consum.* **2018**, *16*, 176–192. [CrossRef]

89. Chiong, M.-C.; Chong, C.T.; Ng, J.-H.; Mashruk, S.; Chong, W.W.; Samiran, N.A.; Mong, G.R.; Valera-Medina, A. Advancements of combustion technologies in the ammonia-fuelled engines. *Energy Convers. Manag.* **2021**, *244*, 114460. [CrossRef]

90. Dimitriou, P.; Javaid, R. A review of ammonia as a compression ignition engine fuel. *Int. J. Hydrog. Energy* **2020**, *45*, 7098–7118. [CrossRef]

91. Frigo, S.; Gentili, R. Analysis of the behaviour of a 4-stroke SI engine fuelled with ammonia and hydrogen. *Int. J. Hydrog. Energy* **2013**, *38*, 1607–1615. [CrossRef]

92. Wang, B.; Li, T.; Gong, F.; Othman, M.H.; Xiao, R. Ammonia as a green energy carrier: Electrochemical synthesis and direct ammonia fuel cell—A comprehensive review. *Fuel Process. Technol.* **2022**, *235*, 107380. [CrossRef]

93. An, X.; Zuo, Y.-Z.; Zhang, Q.; Wang, D.-z.; Wang, J.-F. Dimethyl ether synthesis from CO_2 hydrogenation on a $CuO-ZnO-Al_2O_3-ZrO_2$/HZSM-5 bifunctional catalyst. *Ind. Eng. Chem. Res.* **2008**, *47*, 6547–6554. [CrossRef]

94. Catizzone, E.; Bonura, G.; Migliori, M.; Frusteri, F.; Giordano, G. CO_2 recycling to dimethyl ether: State-of-the-art and Perspectives. *Molecules* **2017**, *23*, 31. [CrossRef]

95. Arcoumanis, C.; Bae, C.; Crookes, R.; Kinoshita, E. The potential of di-methyl ether (DME) as an alternative fuel for compression-ignition engines: A Review. *Fuel* **2008**, *87*, 1014–1030. [CrossRef]

96. Park, S.H.; Lee, C.S. Applicability of dimethyl ether (DME) in a compression ignition engine as an alternative fuel. *Energy Convers. Manag.* **2014**, *86*, 848–863. [CrossRef]

97. Im, J.-Y.; Kim, B.-S.; Choi, H.-G.; Cho, S.M. Effect of pressure for direct fuel cells using DME-based fuels. *J. Power Sources* **2008**, *179*, 301–304. [CrossRef]

98. Kupecki, J. Off-design analysis of a micro-CHP unit with solid oxide fuel cells fed by DME. *Int. J. Hydrog. Energy* **2015**, *40*, 12009–12022. [CrossRef]

99. Zhang, T.; Ou, K.; Jung, S.; Choi, B.; Kim, Y.-B. Dynamic analysis of a PEM fuel cell hybrid system with an on-board dimethyl ether (DME) steam reformer (SR). *Int. J. Hydrog. Energy* **2018**, *43*, 13521–13531. [CrossRef]

100. Sun, D.; Simakov, D.S.A. Thermal management of a Sabatier reactor for CO2 conversion into CH4: Simulation-based analysis. *J. CO_2 Util.* **2017**, *21*, 368–382. [CrossRef]

101. Pasini, G.; Baccioli, A.; Ferrari, L.; Antonelli, M.; Frigo, S.; Desideri, U. Biomethane grid injection or biomethane liquefaction: A technical-economic analysis. *Biomass Bioenergy* **2019**, *127*, 105264. [CrossRef]

102. Transport & Environment. In *Electrofuels? Yes, We can . . . if We're Efficient, Annex II*; Brussels, Belgium, 2020; Available online: https://www.transportenvironment.org/wp-content/uploads/2020/12/2020_12_Briefing_feasibility_study_renewables_decarbonisation.pdf (accessed on 1 February 2023).

103. Ash, N.; Davies, A.; Newton, C. Ricardo Report. In *Renewable Electricity Requirements to Decarbonise Transport in Europe with Electric Vehicles, Hydrogen and Electrofuels*; 2020; p. 4; Ref: ED 13966 Ricardo plc, Shoreham Technical Centre, Old Shoreham Road, Shoreham-by-Sea, West Sussex, BN43 5FG, UK. Available online: https://www.transportenvironment.org/wp-content/uploads/2021/07/2020_Report_RES_to_decarbonise_transport_in_EU.pdf (accessed on 1 February 2023).

104. Moore, C.; Brown, S.; MacDonald, P.; Ewen, M.; Broadbent, H. *European Electricity Review 2022*; Ember: London, UK, 2022.